Glycan:glycan interactions: High affinity biomolecular interactions that can mediate binding of pathogenic bacteria to host cells

Christopher J. Day[a,1], Elizabeth N. Tran[b], Evgeny A. Semchenko[a], Greg Tram[a], Lauren E. Hartley-Tassell[a], Preston S. K. Ng[a], Rebecca M. King[a], Rachel Ulanovsky[a], Sarah McAtamney[a], Michael A. Apicella[c], Joe Tiralongo[a], Renato Morona[b,2], Victoria Korolik[a,2], and Michael P. Jennings[a,1,2]

[a]Institute for Glycomics, Griffith University Gold Coast Campus, Gold Coast, QLD 4222, Australia; [b]School of Biological Sciences, Department of Molecular and Cellular Biology, University of Adelaide, Adelaide, SA 5005, Australia; and [c]Department of Microbiology, University of Iowa, Iowa City, IA 52242

Edited by Rino Rappuoli, GSK Vaccines, Siena, Italy, and approved November 10, 2015 (received for review November 3, 2014)

Cells from all domains of life express glycan structures attached to lipids and proteins on their surface, called glycoconjugates. Cell-to-cell contact mediated by glycan:glycan interactions have been considered to be low-affinity interactions that precede high-affinity protein–glycan or protein–protein interactions. In several pathogenic bacteria, truncation of surface glycans, lipooligosaccharide (LOS), or lipopolysaccharide (LPS) have been reported to significantly reduce bacterial adherence to host cells. Here, we show that the saccharide component of LOS/LPS have direct, high-affinity interactions with host glycans. Glycan microarrays reveal that LOS/LPS of four distinct bacterial pathogens bind to numerous host glycan structures. Surface plasmon resonance was used to determine the affinity of these interactions and revealed 66 high-affinity host–glycan:bacterial–glycan pairs with equilibrium dissociation constants (K_D) ranging between 100 nM and 50 μM. These glycan:glycan affinity values are similar to those reported for lectins or antibodies with glycans. Cell assays demonstrated that glycan:glycan interaction-mediated bacterial adherence could be competitively inhibited by either host cell or bacterial glycans. This is the first report to our knowledge of high affinity glycan:glycan interactions between bacterial pathogens and the host. The discovery of large numbers of glycan:glycan interactions between a diverse range of structures suggests that these interactions may be important in all biological systems.

lipooligosaccharide | lipopolysccharide | glycoconjugates | adherence

Host surface glycosylation is ubiquitous and is targeted by pathogenic bacteria, viruses, fungi and parasites for adherence and toxin binding and by glycosidases (1). *Escherichia coli* type 1 fimbriae, FimH, is one of the most widely studied glycan-recognizing protein adhesins, with specificity for monomannose to oligomannose structures with the variability of the mannose structure bound leading to different tissue tropism (2). Other glycan-recognizing adhesins expressed by bacteria include the following: *Pseudomonas aeruginosa* lectins 1 and 2 (PA-IL and PA-IIL) that have specificity for galactose and fucose, respectively (3); *Helicobacter pylori* SabA, specific for sialic acid containing glycoconjugates including sialyLewis X; and BabA-specific for fucosylated glycoconjugates including Lewis B (4, 5). Although there are numerous known glycan binding adhesins, the adhesins of some bacteria that interact with host surface glycans remain unknown.

Direct interactions between surface glycans (glycan:glycan interactions) have been reported in sea sponges as heterogenous glycan interactions, and in mouse embryo development and cancer where homodimers of Lewis X (LeX) or ganglioside structures play a role in cell adhesion and growth factor receptor interactions (6, 7). Outside of these reports, glycan:glycan interactions, when noted, have generally been considered to be low-affinity, weak interactions (8) that precede high-affinity protein:glycan or protein:protein interactions (1, 2, 5, 9).

Interestingly, there are specific reports of several bacteria expressing truncated surface polysaccharides and oligosaccharides that are significantly less adherent than wild-type equivalents (10, 11), or that their adherence can be blocked by extracted LOS/LPS (10), indicating a role for bacterial surface glycans in adherence to host cells. This decreased adherence of rough strains or blocking of adherence using the free lipooligosaccharide (LOS)/lipopolysaccharide (LPS) in both cell-based and animal infection models has been noted in a range of Gram-negative bacteria including *Campylobacter jejuni*, *Haemophilus influenzae*, *Salmonella typhi*, *Salmonella enterica* serovar Typhimurium, *E. coli*, *Shigella flexneri*, *Pseudomonas aeruginosa*, and *Serratia marcescens* (10, 12–20). Blocking of surface glycans with antibodies has also been shown to inhibit adherence and invasion of cell layers in a range of bacteria, including *S. flexneri* (21–23). The cellular receptors for adherence via these bacterial surface glycans have not been identified. To address the hypothesis that there may be direct interactions between bacterial and host glycans that mediate adherence, we conducted glycan microarray screening of four different species

Significance

Pathogens use cell surface carbohydrates as a means of attachment to host tissues. In several pathogenic bacteria, truncation of surface carbohydrates, lipooligosaccharide, or lipopolysaccharide have been reported to significantly reduce bacterial adherence to host cells. Here, we show that the lipooligosaccharide/lipopolysaccharide of four distinct bacterial pathogens bind directly to a range of host glycans. Surface plasmon resonance data confirmed binding among 66 different host–glycan:bacterial–glycan pairs. We also demonstrated that bacterial adherence can be competitively inhibited by either host cell or bacterial glycans. Our discovery of high-affinity glycan:glycan interactions in infectious disease may provide new approaches for therapy and prevention. The discovery of the existence of extensive, high-affinity interactions between glycans will alter the perception of the importance of these macromolecular interactions in all biological systems.

Author contributions: C.J.D., E.N.T., M.A.A., J.T., R.M., V.K., and M.P.J. designed research; C.J.D., E.N.T., E.A.S., G.T., L.E.H.-T., P.S.K.N., R.M.K., R.U., S.M., and M.P.J. performed research; M.A.A. and R.M. contributed new reagents/analytic tools; C.J.D., E.N.T., E.A.S., G.T., L.E.H.-T., P.S.K.N., R.M.K., J.T., R.M., V.K., and M.P.J. analyzed data; and C.J.D., E.N.T., R.M., V.K., and M.P.J. wrote the paper.

The authors declare no conflict of interest.

This article is a PNAS Direct Submission.

Freely available online through the PNAS open access option.

[1]To whom correspondence may be addressed. Email: c.day@griffith.edu.au or m.jennings@griffith.edu.au.

[2]R.M., V.K., and M.P.J. contributed equally to this work.

This article contains supporting information online at www.pnas.org/lookup/suppl/doi:10.1073/pnas.1421082112/-/DCSupplemental.

of pathogenic bacteria with well-characterized surface glycan structures: *C. jejuni*, *H. influenzae*, *S. typhimurium*, and *S. flexneri.* These studies included whole live bacteria expressing wild-type and LOS/LPS truncation mutants, as well as purified LOS/LPS from the same set of bacteria.

Results

Bacterial LOS/LPS Recognize Host Surface Glycans and Truncations of These Structures Reduce/Alter Binding. Fluorescently labeled whole bacterial cells from all four species bound to many structures on the glycan microarray, including blood group and Lewis antigens and glycosaminoglycans (Figs. 1 and 2 and Dataset S1). The total number and diversity of glycans bound by these bacteria were reduced when the surface glycans (LOS/LPS) were truncated by mutation. The truncated LOS/LPS mutant bacteria of *S. flexneri* RMA2161 (containing an Δ*rmlD* mutation; 44 structures bound by wild-type reduced to 13 for Δ*rmlD*), *C. jejuni* (Δ*waaF*; 104 structures bound by *C. jejuni* wild-type grown at 42 °C to 2 structures bound by Δ*waaF*), and *S. typhimurium* bound fewer than half the structures observed for wild-type bacteria (180-Δ*galE*; 89 structures bound by wild-type reduced to 27 in 180-Δ*galE*), whereas the loss of sialic acid from *H. influenzae* Δ*siaP* LOS altered the types of glycans recognized by these cells (Figs. 1 and 2 and Dataset S1). To test for a direct role of these LOS/LPS structures in adherence of the bacteria to the glycans on the microarray, the glycan microarray studies were repeated by using purified LOS/LPS from this same set of bacterial strains. The fluorescently labeled LOS/LPS structures bound to a large proportion of the same subset of glycan structures bound by the equivalent whole bacterial cells (Figs. 1 and 2 and Dataset S1). This data suggest that a significant proportion of the glycan binding observed in whole cells is mediated by bacterial surface glycans.

Surface plasmon resonance (SPR) was used to examine direct binding among 80 different host–glycan:bacterial–LOS/LPS–glycan pairs identified in the glycan microarray studies. Of the interactions tested, 31 had affinities (equilibrium dissociation constant; K_D) in the range of 140 nM–50 μM (Fig. 3, Tables S1–S4, and Dataset S2). Interactions with K_D values less than 50 μM are comparable to typical values observed for binding between lectins or antibodies and glycans (2, 3, 24). For *S. flexneri*, wild-type 2a LPS, the highest affinity interaction was observed with the A blood group antigen with a K_D of 0.81 μM, whereas *C. jejuni* 11168 LOS bound with the highest affinity to the B blood group antigen (K_D = 0.14 μM; Fig. 3 and Tables S1 and S2). *S. typhimurium* was found to have 1.89–2.59 μM affinity for four different structures including all three ABO blood groups and LewisX (Fig. 3 and Table S3), whereas *H. influenzae* showed higher affinity binding to Lewis A antigen (8 μM) than ABO blood group antigens (42–80 μM; Fig. 2 and Table S4). Interestingly, for *S. flexneri*, the increasing numbers of repeat units of the O-antigen subunits in LPS corresponded to increased binding constant, with 2–6 repeats or fewer displaying reduced affinity for all structures tested (Table S2). *C. jejuni* LOS displayed the highest affinity interaction observed in this study with a 140 nM K_D for binding to blood group B tetrasaccharide. Binding of *C. jejuni* LOS to negatively charged glycans, such as chondroitin sulfate, was 100-fold stronger when sialic acid was absent from the *C. jejuni* LOS molecule, suggesting that sialic acid and other negatively charged components of glycans, including sulfation, may inhibit or reduce the affinity of glycan:glycan interactions (Fig. 3 and Table S1).

To determine whether the 31 high-affinity interactions described above solely depended on the glycan components of LOS and LPS and not due to or reliant on the lipid A portion of the molecules, modified O-deacylated LOS/LPS were generated from the purified LOS/LOS. The resulting O-deacylated oligo/polysaccharides have no lipid A, and the nonreducing end of the structures terminate after the KDO residue. Using established

Bacteria	LOS/LPS Structure
C. jejuni 11168-O*	$^{(+/-)}$Neu5Acα(2-3) | Galβ(1-3)GalNAcβ(1-4)Galβ(1-3)Galβ(1-3)Hepα(1-3)Hepα(1-5)**Kdo-LipidA**
C. jejuni 11168-O Δ*cgtA/neuA*	Galβ(1-3)Galβ(1-3)Hepα(1-3)Hepα(1-5)**Kdo-LipidA**
C. jejuni 11168-O Δ*waaF*	Hepα(1-5)**Kdo-LipidA**
C. jejuni 11168-O Δ*wlaA-wlaT*	**Kdo-LipidA**
Shigella flexneri RMA2159	(3/4)Ac Glc α(1-4) (6)Ac | | | $_n$[→2)Rhaα(1-2)Rhaα(1-3)Rhaα(1-3)GlcNAcβ(1-3)]Glcα(1-3)Galα(1-3)Glcα(1-3)Hepα(1-3)Hepα(1-5)Kdo-**Kdo-LipidA**
Shigella flexneri RMA4328	(3/4)Ac Glc α(1-4) (6)Ac | | | $_{n=2\text{-}6}$[→2)Rhaα(1-2)Rhaα(1-3)Rhaα(1-3)GlcNAcβ(1-3)]Glcα(1-3)Galα(1-3)Glcα(1-3)Hepα(1-3)Hepα(1-5)Kdo-**Kdo-LipidA**
Shigella flexneri RMA2161	Glcα(1-3)Galα(1-3)Glcα(1-3)Hepα(1-3)Hepα(1-5)Kdo-**Kdo-LipidA**
S. typhimurium 180	OAc-(2)Abeα(1-3) GlcNAcα(1-2) Galα(1-6) | | | $_n$[2-)Manα(1-4)Rhaα(1-3)Galα(1]-4)Glcα(1-2)Glcα(1-3)Glcα(1-3)Hepα(1-3)Hepα(1-5)**Kdo-LipidA**
S. typhimurium 180 Δ*galE*	Hep α(1-3)Hepα(1-5)**Kdo-LipidA**
H. influenzae 2019#	(4)OAc PPEtn(-4) | | ChoP(-6)Glcβ(1-4)l-Hep(α1-5)(P)**Kdo-LipidA** | PPEtn(-6)Hepα(1-3) | Neu5Acα(2-3)Galβ(1-4)Glc(OAc)α(1-2)Hep(OAc)α(1-2)
H. influenzae 2019 Δ*siaP*#	(4)OAc PPEtn(-4) | | ChoP(-6)Glcβ(1-4)l-Hep(α1-5)(P)**Kdo-LipidA** | PPEtn(-6)Hepα(1-3) | Galβ(1-4)Glc(OAc)α(1-2)Hep(OAc)α(1-2)

Fig. 1. Structures of LOS/LPS used in this study. LOS/LPS structures of the organisms used in this study. *, *C. jejuni* 11168-O is 90% sialylated at 37 °C and less than 50% at 42 °C (59). The underlined section is the terminal structure used in the ITC experiment. #, *H. influenzae* 2019 LOS is phase variable only one product is shown (60).

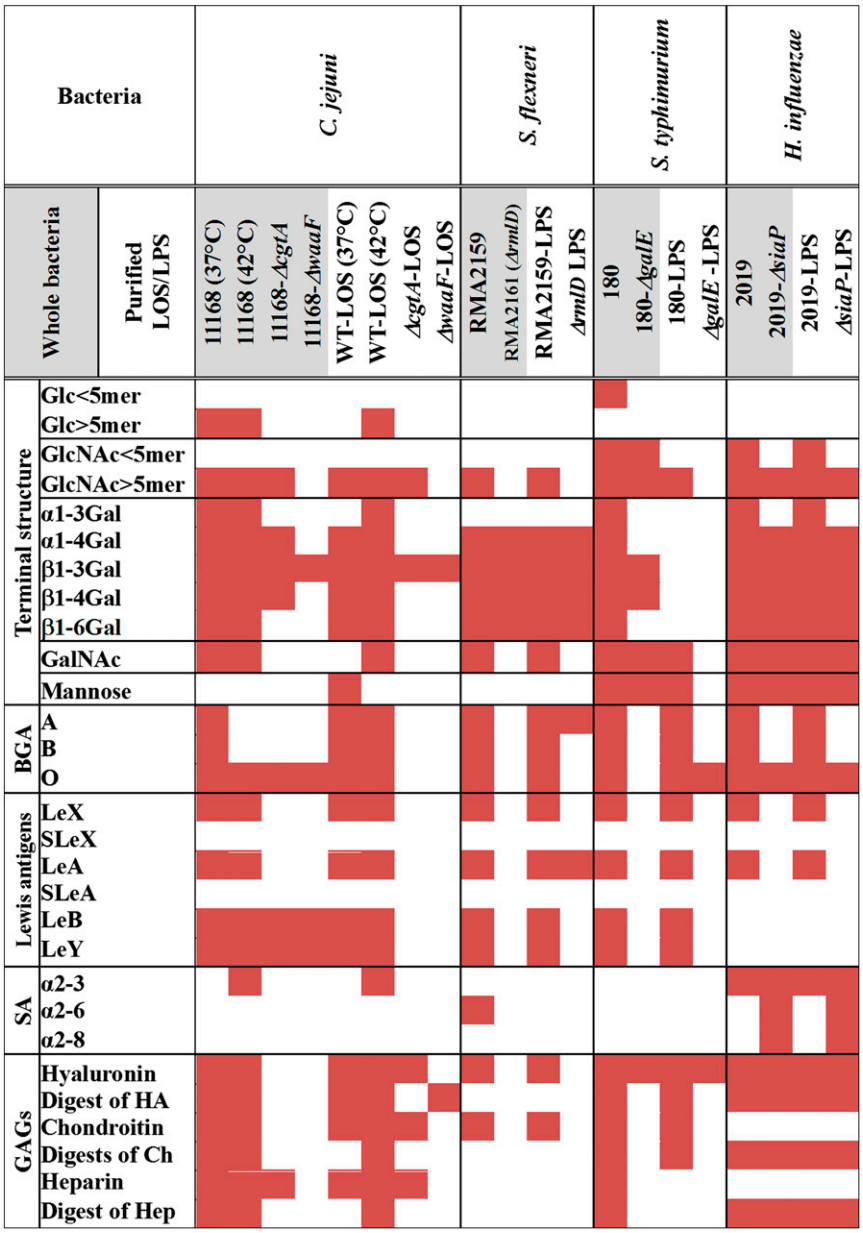

Fig. 2. Analysis of LPS/LOS glycan interactions with glycan array and SPR. Heat map of glycan binding from glycan array and SPR experiments. Comparison between whole bacteria and isolated LOS/LPS molecules. Binding to glycans on the array have been grouped into common terminating structures; for a full list of binding to individual structures see Dataset S1. Interactions are noted in red for binding or white if no binding was observed by glycan array analysis.

methods (25, 26), a primary amine was added to the nonreducing end KDO, and this primary amine was used to covalently link the O-deacylated oligo/polysaccharides CM7 SPR sensor chips. These linked glycans were then analyzed by SPR to determine the affinity of host–gycan:bacterial–glycan interacting pairs. All 31 high-affinity interactions described above retained high-affinity interactions with their respective host glycans after removal of the lipid A portion of LOS/LPS. This data supports the hypothesis of existence of direct interactions between bacterial and host glycans. In general, the affinities between the host–gycan:bacterial–glycan pairs were improved by removal of the lipid A (Fig. 3 and Tables S1–S4), with an additional four pairs moving from the low-affinity interaction category into the sub-50 μM K_D range.

The highest affinity interaction observed in these SPR studies was between *C. jejuni* LOS and the human blood group B structure (Fig. 4). The terminal antennae *C. jejuni* LOS is a molecular mimic of the human ganglioside structure asialo-G_{M1}. Isothermal calorimetry (nano-isothermal titration calorimeter) was performed on commercially sourced, chemically synthesized asialo-G_{M1} and the blood group B tetrasaccharide (Fig. 4 and Fig. S1). The ITC analysis revealed a K_D of 98 nM (±21 nM) (Fig. 4 and Fig. S1). This affinity measurement is not significantly different to the values obtained from SPR for LOS and O-deacylated LOS (Fig. 3 and Table S1; $P = 0.062$).

Adherence of Bacterial Pathogens To Host Cells Can Be Inhibited with Free Glycans from Host or Bacteria. To analyze the potential of LOS/LPS mutations and glycan:glycan interactions to mediate bacterial adhesion to host cells, cell association assays were performed with *C. jejuni, S. typhimurium, H. influenza*, and *S. flexneri* (Fig. 5).

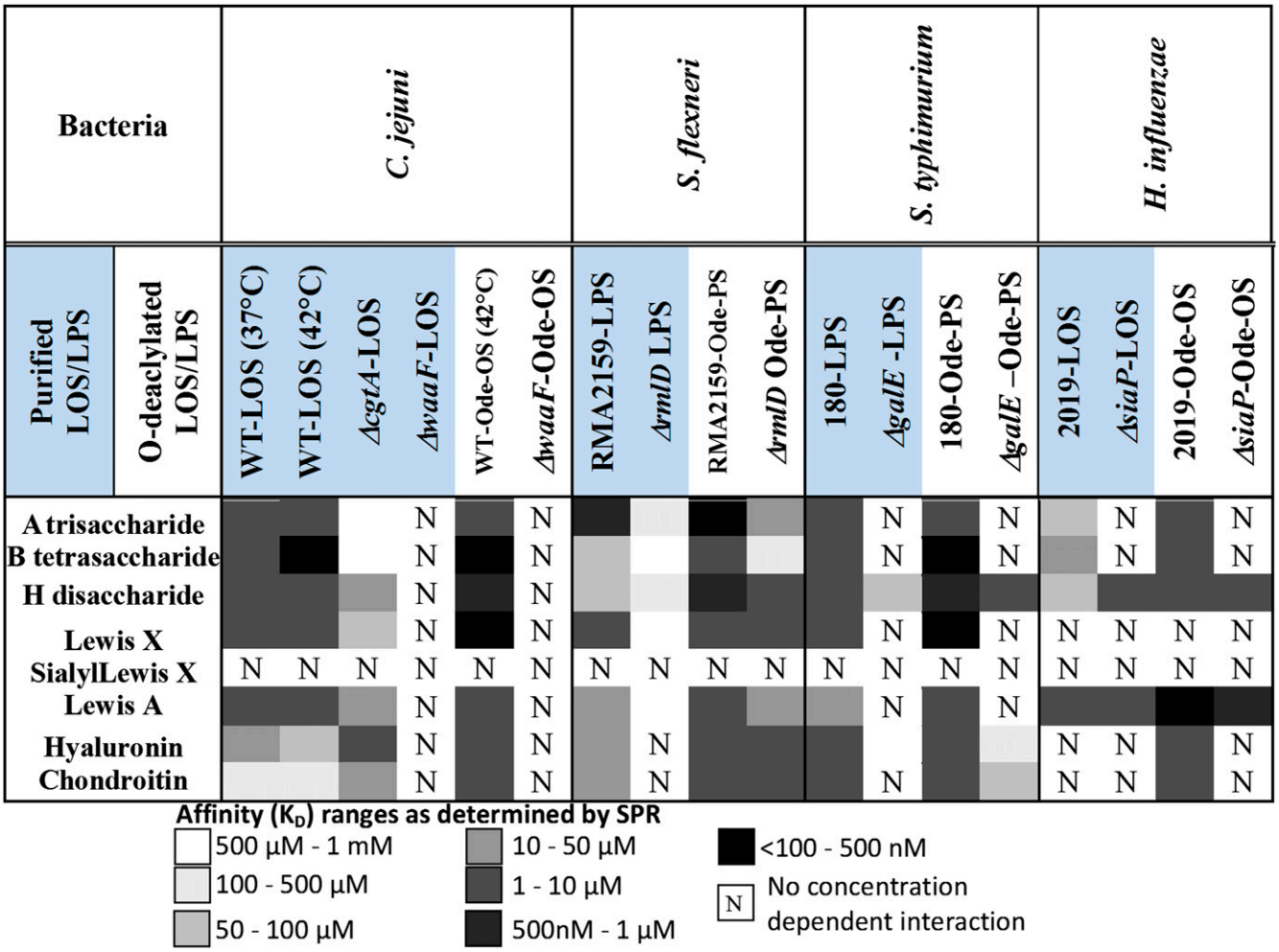

Fig. 3. Analysis of affinities of interactions between bacterial LOS/LPS structures and free host glycans by SPR. Heat map of affinities of binding between bacterially derived LOS/LPS structures with various host glycans. Measurements were done with whole LOS/LPS and amine-modified O-deacylated LOS/LPS glycans. Increased affinity is indicating by a darker color (see key). A white box with an "N" indicates that no concentration-dependent interaction could be identified. Full K_D measurements can be found in Tables S1–S4.

Adherence of *C. jejuni* to Caco-2 intestinal epithelial cells could be inhibited by free glycans from both host cell (free host glycans) and bacterial (free bacterial glycans) surfaces in a dose-dependent manner (Fig. 5*A*). Inhibition of *C. jejuni* adherence to Caco-2 cells by host glycans was consistent with the hierarchy of structural interactions as determined by SPR (Fig. 2 and Table S1), with the blood group B trisaccharide (K_D = 0.14 μM) inhibiting most effectively, followed by the O (H-) disaccharide (K_D = 1.4 μM) and the A trisaccharide (K_D = 8.0 μM; Fig. 5*A*). *C. jejuni* cell association could also be inhibited with free bacterial glycan, because a significant reduction in adherence was observed in the presence of *C. jejuni* 11168-O O-deacylated LOS oligosaccharide (*C. jejuni* OS) at a concentration of 3.3 μM, but not by 0.33 μM of the *C. jejuni* OS (Fig. 5*A*). The Caco-2 cells used in the *C. jejuni* assays are known to express O-blood group antigen (27). This surface expression of blood group antigen by the Caco-2 cells is consistent with the cell association studies, because the A-blood group showed little inhibition. The affinity of the *C. jejuni* for A-blood group glycan is lower than the O-blood group glycan expressed on the surface of the Caco-2 cells. We also observed inhibition of adherence of *C. jejuni* to Caco-2 cells in the presence of either an anti-blood group O antibody or anti-G_{M1} antibody (bacterial surface glycan), but not with a negative control anti-blood group A antibody (Fig. 5*D*). The blood group antibodies do not cross-react at high affinity with other blood group antigens or nonfucosylated terminal galactose or GalNAc structures, making the blood group A antibody a good low-affinity negative control for Caco-2 cells in this assay.

Inhibition of cell association was observed for *S. flexneri* in assays with T84 epithelial cells known to express the carcinoembryonic antigen (28), with the blood group A-trisaccharide, which had the highest affinity for *S. flexneri* LPS in SPR analysis (K_D = 0.81 μM), inhibiting adherence to T84 cells better than the blood group B or blood group H structures (both K_D ~80 μM; Figs. 2 and 5*B* and Table S1). Both the complete LPS and O-deacylated (polysaccharide component only) LPS significantly reduced the adherence of *S. flexneri* to T84 cells (Fig. 3*C*). To investigate the ability of smooth LPS (S-LPS) and rough LPS (R-LPS) *S. flexneri* 2a bacteria to adhere to epithelial cells in the presence of different competing glycans, polarized T84 cells were initially infected with strains RMA2159 (S-LPS) and RMA2161 (R-LPS) in the presence of equivalent mass concentrations of *S. flexneri* LPS and *S. flexneri* O-deacylated LPS (S-PS). The results of Fig. 5 show that in the absence of any competing glycan (untreated), smooth RMA2159 adheres significantly to T84 cells ~3× more than rough RMA2161 bacteria ($P < 0.0001$) (Fig. 5*C*). The calculated percentage adherence of smooth RMA2159 and rough RMA2161 to T84 cells was 0.342% and 0.104% of the

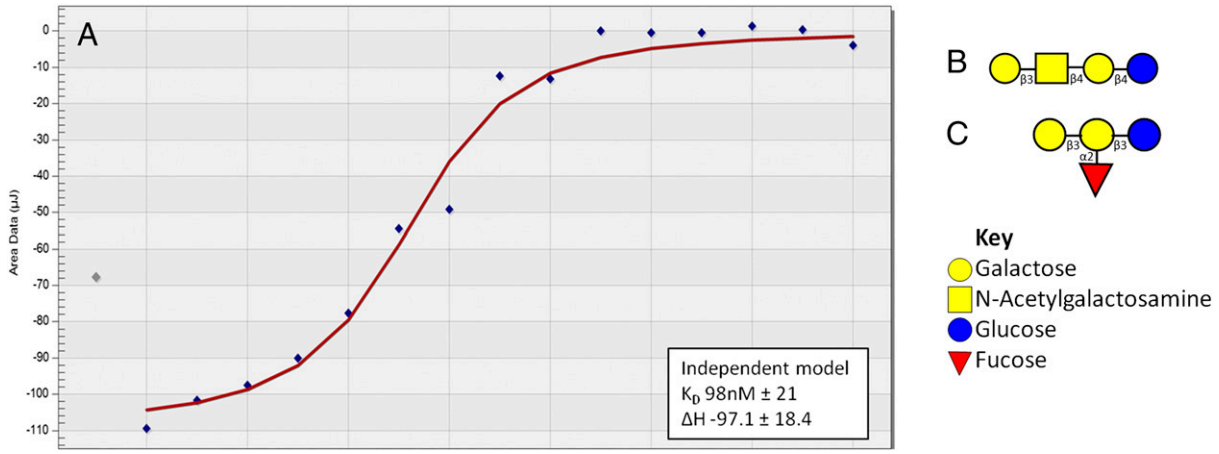

Fig. 4. (*A*) Analysis of interactions between synthetic glycans of structures matching *C. jejuni* terminal LOS structure [asialoG_{M1}]; (*B*) and blood group B tetra saccharide (*C*) by isothermal calorimetry. Sigmoidal fit of the interaction with self interactions for aG_{M1} and blood group B and heat of injection subtracted.

initial inoculum, respectively. In the presence of competing glycan, S-LPS showed the highest inhibition of bacterial adherence, whereas R-LPS still showed significant inhibition of both bacterial strains (Fig. 5*C*). These results suggest that there are glycan receptors for both S-LPS and R-LPS on the cell surface of T84. In the presence of O-deacylated LPS (S-PS), adherence of smooth RMA2159 was inhibited but not rough RMA2161, further suggesting that there are two separate cell receptors (Fig. 5*C*). The presence of equivalent molarity (4.3 μM) of each competing glycan was also tested and a similar trend was observed (Fig. 5*C*). Interestingly, data represented in Fig. 5 show that in the absence of competing glycan, the ratio of RMA2159:RMA2161 adherence is 3:1, but in the presence of 4.3 μM S-LPS, 7.4 μM R-LPS, or 0.32 μM S-PS, the RMA2159:RMA2161 adherence ratio was reduced to ∼1:1 (Fig. 5). When equivalent molarity (4.3 μM) of each competing glycan were used, 4.3 μM of S-LPS gave a ratio of 1.2:1, 4.3 μM of R-LPS gave a significant ratio of 3:1, and 4.3 μM of S-PS gave a significant ratio of 0.4:1, suggesting that the oligosaccharide component of S-LPS plays an important role in *S. flexneri* adherence to cells ($P < 0.0001$) (Fig. 5*C*).

The ability of RMA2159 and RMA2161 to adhere to epithelial cells in the presence of A, B, and O blood group oligosaccharides was also performed (Fig. 5*B*). In the presence of increasing K_D concentrations of A trisaccharide, the ratio of RMA2159:RMA2161 adherence was gradually reduced from 3:1 (untreated) to 0.9:1 (10× K_D), suggesting that A trisaccharide competes for the same receptor as smooth RMA2159. In the presence of B trisaccharide, an effect on smooth RMA2159 adherence was only observed at the highest 10× K_D concentration (ratio of ∼1:1), whereas the presence of O (H-) disaccharide did not have much effect on smooth RMA2159 adherence to T84 (ratio of ∼2.5:1 at all K_D values tested). Overall, these results suggest that the oligosaccharide component of S-LPS may interact with glycan receptors and also bind A trisaccharides.

Using fluorescently labeled *S. flexneri* type 2a O-deacylated polysaccharide, we observed specific binding to cells located in intestinal glands of the human ileum (Fig. 6), consistent with the data of Arena et al (29). The Alexa-488 labeled polysaccharide shows clear overlap with a monoclonal antibody to glycoprotein 2 (GP2), an M-cell specific marker (Fig. 6, 2–6), and indicates that the polysaccharide-only portion of the LPS of *S. flexneri* is sufficient to bind to the known cell target of *S. flexneri* (30), and colocalizes with a protein that expresses a large amount of glycosylation, including fucosylated structures (31–33). Fucosylated structures were noted as a target for *S. flexneri* LPS in our array and SPR analysis.

For *S. typhimurium* adhering to Caco-2 cells, significant reduction in adherence was observed when using 10× the K_D for the three blood group antigens (18.9–25.9 μM; Fig. 5*E*). Significant reduction in *S. typhimurium* was also noted in the presence of the blood group A and blood group O host glycans ($P < 0.05$) but not in the presence of the B blood group glycan (Fig. 3*E*).

Association of *H. influenzae* To Host Cells Correlates with Changes to LOS Structure. To test the role of LOS structural length in cell association, a range of *H. influenzae* LOS mutants was tested for changes in association to the bronchial epithelial cells 16HBE14. *H. influenzae* 2019 producing a full-length LOS (Fig. 1) had 12.6% of the inoculum associating with cells at 2 h (Fig. 5*F*). *H. influenzae* Δ*siaP*, producing a full-length LOS that is not sialylated, had 46.4% of the inoculum associated with cells at 2 h, significantly more than the sialylated wild type. These data demonstrate that alterations to the LOS structure of *H. influenzae* can dramatically change the total number of bacteria associating with 16HBE14 cells. Interestingly, like *H. influenzae* Δ*siaP*, when using the sialic acid knockout *C. jejuni* 11168 Δ*cgtA*/*neuB*, adherence almost doubled compared with wild-type *C. jejuni* 11168-O (Fig. 5*A*).

Discussion

Reports of direct glycan:glycan interactions in the literature have been limited to examples of sea sponge cell:cell interactions and LeX:LeX histocompatibility antigens and ganglioside interactions (6, 7). Glycan:glycan interactions in sea sponges have been shown to play a role in the disassembly and reassembly of the complex three-dimensional structure of the sea sponge, realigning based on the surface glycans of each cell type and their neighboring cells (7, 34). LeX:LeX interactions have been noted in embryo development in mice. Blocking LeX:LeX interactions with anti-LeX antibodies was shown to inhibit cell–cell interactions (6). It has also been noted through the use of atomic force microscopy that, in sea sponges, the glycan:glycan interactions between two adjacent cells can be as strong as interactions between antibodies and antigens (34). The strength of these interactions has been ascribed to the polyvalency of these abundant surface glycans. LeX–LeX interactions have been assessed by using SPR and were shown to have an affinity of 0.54 μM (35), which is within the ranges we have detected here for a much broader screen of glycan:glycan interactions.

In this study, we have observed direct interactions between single bacterial LOS/LPS molecules and single host glycans with K_D values in the high nanomolar to low micromolar range. The

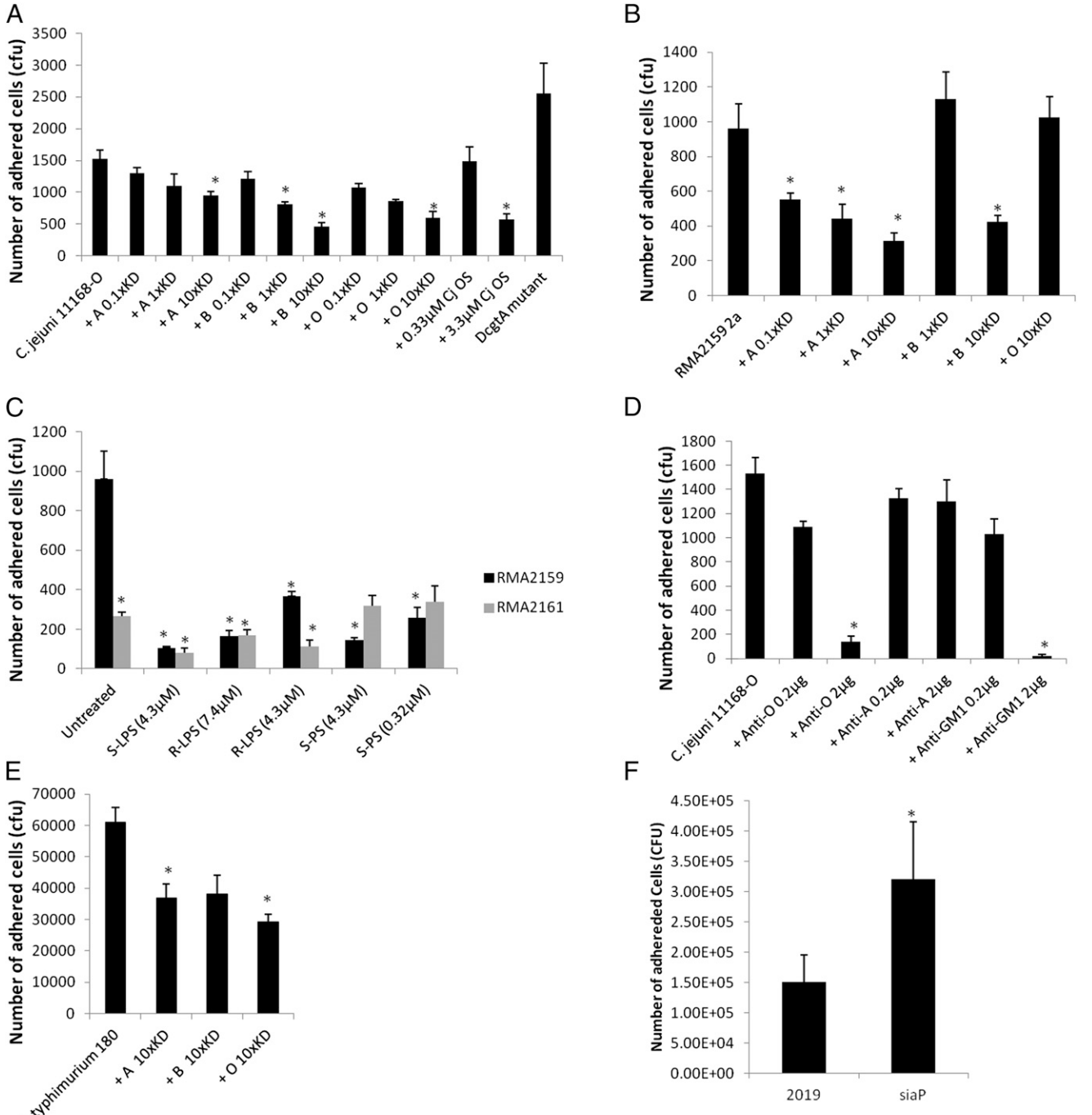

Fig. 5. Adherence assays in the presence of free host or bacterial glycans. (*A*) *C. jejuni* 11168-O wild-type adherence to Caco-2 epithelial cells in the presence or absence of free blood group antigens (A-trisaccharide 0.8 μM, 8 μM, 80 μM; B-trisaccharide 0.014 μM, 0.14 μM, 1.4 μM; or H-disaccharide 0.14 μM, 1.4 μM, 14 μM); *C. jejuni* 11168-O 42 °C LOS oligosaccharide (Cj OS) at 0.33 and 3.3 μM. (*B*) *S. flexneri* adherence to T-84 epithelial cells in the presence or absence of free blood group antigens (A-trisaccharide 0.08 μM, 0.81 μM, 8.1 μM; B-trisaccharide 84.9 μM, 849 μM or H-disaccharide 803 μM). (*C*) *S. flexneri* adherence to T-84 epithelial cells in the presence or absence of free bacterial oligo/polysaccharides Sf S-PS (0.32 or 4.3 μM) or Sf S-LPS (4.3 μM) or Sf R-LPS (7.4 or 4.3 μM). (*D*) *C. jejuni* adherence to Caco-2 epithelial cells in the presence or absence of antibodies to cell and bacterial surface glycans (A and O blood group antigens and G_{M1} ganglioside) at 0.2 and 2 μg/mL. The O blood group antibody will target the O-blood group antigen on the surface of Caco-2 cells with high affinity, the A blood group antibody will target the O blood group and nonfucosylated α-GalNAc structures on the Caco-2 cells with low affinity and the anti-G_{M1} antibody will target structures on the Caco-2 cells and *C. jejuni* 11168-O (G_{M1} mimic) with high affinity. (*E*) *S. typhimurium* 180 and Caco-2 cells in the presence or absence of free blood group antigens (A-trisaccharide 26 μM; B-trisaccharide 21 μM; or H-disaccharide 19 μM). (*F*) Cell association between *H. influenzae* LOS mutants and 16HBE14 bronchial epithelial cells expressed as a percentage of the original inoculums at 2 h. *H. influenzae* WT (2019); *H. influenzae* Δ*siaP* (siaP). *, significant difference compared with untreated/wild-type control.

nature of these interactions is not known; however, glycan:glycan interactions involving intermolecular hydrogen bonding have been noted in simple glycan crystals, with sucrose known to have up to six intermolecular hydrogen bonds within a crystal (36), and glucose forming two hydrogen bonds in a glucose crystal (37). Chitin forms two interchain hydrogen bonds between the C=O

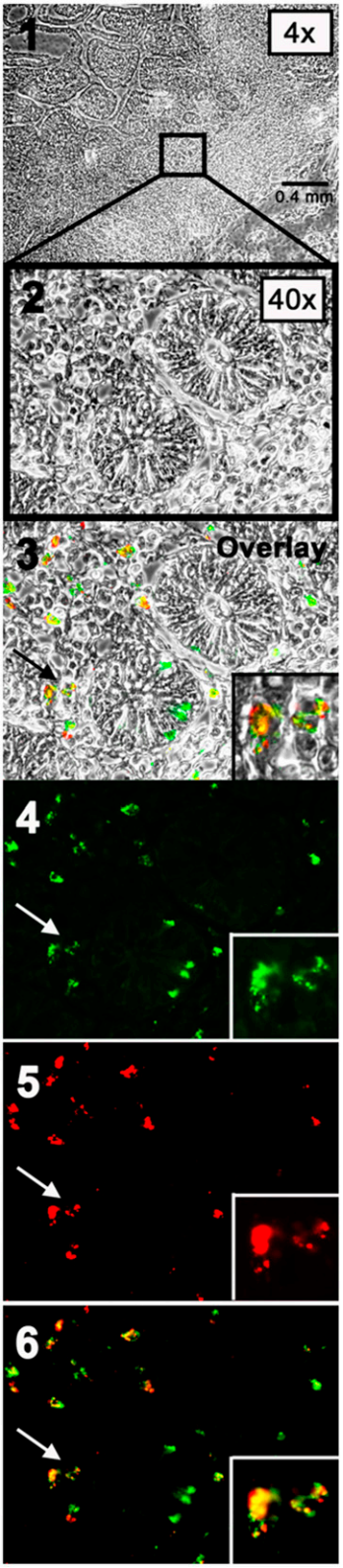

Fig. 6. Labeling of human small intestines shows colocalization of *S. flexneri* type 2a Alexa 488-polysaccharide and the M-cell marker anti-GP2. Human ileum section viewed at 4x (*1*) and 40x objectives with phase contrast optics (*2* and *3*). At 40x, cells were also viewed under fluorescence for Alexa 488-polysaccharide (*4*; green) and GP2 (*5*; red). Overlay images (*3* and *6*) show areas of colocalization in yellow. Arrows point to cells enlarged for better clarity (bottom corner of each frame).

and NH groups and/or the C6-OH of neighboring sugars (38). There are also no fewer than 16 hydrogen bonds between neighboring lactose molecules in a lactose crystal, and this large number of bonds is used to explain the hardness of the lactose crystal (39). In polymers like DNA, these cumulative hydrogen binding interactions result in a highly stable structure due to the length of the molecule. Glycan:glycan interactions have the potential to form similarly stable structures because of carbohydrate chain length of single polymer molecules (e.g., lipopolysaccharide in bacteria), or the valiancy resulting from the thousands of individual glycans present on the surface of every cell.

A handful of previous studies have identified glycolipid:glycolipid or glycan:glycolipid interactions in eukaryotic systems (6, 7, 34, 35). In this study, we initially demonstrated numerous high-affinity LOS/LPS:host–glycan interactions by SPR. Together these data suggested glycan:glycan binding may be mediating the high-affinity interactions observed between these biomolecules. However, in each case, a lipid component is present. For example, lipid A on LOS/LPS or the ceramide lipid attached to the glycan of a ganglioside. It is possible that the lipid component of these biomolecules may be involved in these interactions. To exclude this possibility, we prepared and tested O-deacylated oligo/polysacchrides in our glycan:glycan interactions studies. The initial screening of the lipid A containing LOS/LPS with host glycans identified 31 host glycan:LOS/LPS pairs with affinities less than 50 μM; all 31 of these interactions were retained with affinities less than 50 μM when the lipid A was removed. Not only were the 31 highest affinity interactions confirmed, but in general, the affinities between glycans and O-deacylated oligo/polysaccharides were higher than those observed for glycans and LOS/LPS. These data support the hypothesis that the host glycans are responsible for direct interactions with the glycan portions of bacterial surface LOS/LPS structures.

Previous studies of these four pathogens have linked LOS/LPS to adherence/virulence with full-length LOS/LPS for each of these organisms is absolutely required for virulence in animal models (40–43). *S. flexneri* LPS O-antigen is a virulence factor whose chain length affects both serum resistance and the function of surface virulence factors; a role for LPS in cell invasion has been reported (11, 44-46). *S. flexneri* infection has also been blocked by both the addition of free LPS and treatment with anti-LPS antibodies (11, 14, 21). These studies are a strong indication that the LPS of *S. flexneri* is a key factor in adherence and virulence. Interactions of *S. flexneri* LPS with host glycans, as demonstrated here with glycan array and SPR, and that free glycans from both host and bacteria can block more than 60% of total bacteria:host–cell association. The fact that both the host and bacterial glycans inhibited cell association is a strong indication that these two glycans are interrupting the same interaction; i.e., that the adherence of this bacteria to host cells depends on glycan:glycan binding between the LPS and the host surface glycome. Also the observation that blocking of adherence by using the three blood group antigens follows the recorded affinities of the *S. flexneri* polysaccharide for these host structures adds further evidence to support the role of glycan:glycan interactions. In terms of the pathogenesis of *S. flexneri,* binding to host cells is not sufficient for invasion because the type-3 secretion system is needed. However, as stated by Köhler et al. that *S. flexneri* interaction with the basolateral membrane domain of polarized cells results in a mucosal inflammatory immune response that is polysaccharide dependent (11) and, therefore, based on this study may be glycan:glycan in nature. We have shown direct interaction between the *S. flexneri* type 2a polysaccharide and GP2 on M cells in human ileum tissue sections. GP2 is a heavily glycosylated protein that is an established marker for M cells (47). Before the use of the GP2 antibody, this protein was identified on M cells with UEA-1, a lectin with specificity for the α1–2-linked fucose structures found in the

blood group antigens on this glycoprotein (33, 47–49). The interaction of *S. flexneri* polysaccharide with GP2 provides further evidence for a polysaccharide-dependent adherence mechanism for *S. flexneri* that is likely to involve binding to host glycoconjugates identified in our array screen and confirmed with SPR.

For *C. jejuni*, the most comprehensive studies of the role of LOS in infection has been performed with the strain *C. jejuni* 81–176. The results of mutations to the *C. jejuni* 81–176 LOS length have varied; mutagenesis of *cgtA* lead to increased invasion of cell layers, whereas large truncation mutants had decreased invasion (50, 51). In our study, adherence of the *C. jejuni* 11168 Δ*cgtA*/*neuB* was increased compared with wild type. This increase may be due to removal of sialic acid from the LOS structure, because it has been reported previously that when Caco-2 cells are sialidase treated, adherence of wild-type *C. jejuni* 11168 doubles (52). As well as the O-blood group antigen, Caco-2 cells also express GAGs (53), which would provide binding sites for 11168 Δ*cgtA*/*neuB* with higher affinity than the wild-type *C. jejuni* 11168. Unfortunately, direct comparison between the *C. jejuni* 81–176 Δ*cgtA* mutant and the *C. jejuni* 11168 Δ*cgtA*/*neuB* mutant used in this study is not possible, because the *cgtA*/*neuB* in *C. jejuni* 11168 is a bifunctional enzyme involved in the synthesis of CMP-Neu5Ac and the translocation of GalNAc (24). From the results obtained in this study for *C. jejuni*, it appears that the terminal galactose and *N*-acetylgalactosamine are required for high-affinity interactions with blood group and Lewis antigens, but actually inhibit interactions with GAGs (Table S1). Interestingly it has already been noted that free host glycans, such as breast milk glycans and H(O-) antigens, can inhibit *C. jejuni* infection (54) and be used as a defense against pathogenic bacteria. However, no *C. jejuni* surface receptor for these glycans has been identified. Our results support this data and suggest a mechanism of action of breast milk glycans inhibiting infection maybe through glycan:glycan interactions.

S. typhimurium LPS is also a major virulence factor with the length of the O-antigen contributing to survival in the host (40, 55) and has been shown to play a role in adherence (56). We found that host blood group glycans could inhibit the association of *S. typhimurium* and Caco-2 cells when used at 10× the K_D of the LPS:glycan interaction with 50% decreases in adherence noted. We have shown that the LPS and the O-deacylated polysaccharide of *S. typhimurium* can interact directly and that blood group antigens free in solution may be inhibiting LPS-mediated adherence.

H. influenzae showed the lowest affinity for blood group antigens, instead preferring Lewis structures. In adherence assays, the mutant lacking sialic acid (Δ*siaP*) showed increased adherence. The LOS isolated from the *H. influenzae* Δ*siaP* mutant also had eightfold or greater affinity for Lewis A and blood group O glycans compared with that of wild-type LOS (Table S1) in agreement with the increased adherence phenotype. This increased adherence for *H. influenzae* Δ*siaP* also supports the data observed for *C. jejuni*, where removal of sialic acid increased bacterial adherence to host cells. It is interesting to note that negative charges on glycans can significantly reduce, inhibit, or alter the types of structures involved in the glycan:glycan interactions we have observed. It has been noted that sialic acid is an important component expressed by red blood cells and metastatic cancer cells and functions to inhibit direct interaction of cells through charge repulsion (57, 58).

This study is the first report to our knowledge of extensive, high-affinity, glycan:glycan interactions in biological systems. We report more than 60 previously unidentified bacterial–glycan: host–glycan high-affinity interactions, suggesting that glycan: glycan interactions may be a widespread phenomenon rather than being limited to the small number of interactions shown previously (6, 7, 34). Our discovery may be used to guide development of novel antiinfective therapeutics, vaccines, and glycan-based molecular probes. Moreover, it is important to note that *C. jejuni* and *H. infleunzae* LOS glycans are archetypal examples of host molecular mimicry. These organisms express multiple glycans on their LOS that are identical to human glycoconjugates (e.g., G_{M1} and asialo-G_{M1} on *C. jejuni* LOS; refs. 24 and 59). The high-affinity glycan:glycan interactions observed in Fig. 4, suggests that glycan:glycan interactions may also mediate mammalian cell:cell interactions on a much broader scale and at a higher affinity than previously thought. Therefore, the discovery of high-affinity glycan:glycan interactions in host: pathogen biology has the potential to impact our understanding of these interactions in a wide range of biological systems.

Materials and Methods

Bacterial Strains and Growth Conditions. The *S. flexneri* strains used in this study are all derived from *S. flexneri* 2457T (serotype 2a) and are cured of the virulence plasmid (VP-ve) and, hence, are noninvasive in HeLa cell monolayers. They are as follows: RMA2159 (S-LPS), RMA2161 *rmlD::kan*^{r} (R-LPS), and RMA4328 [pHS2 *wzz*$_{pHS2}$::Tn*5*-Cml/*wzz*::kan^r, carrying pRMCD76 which encodes *wzz*$_{O139}$(*otnB*)] (VS-LPS). *C. jejuni* 11168-O was sourced from Diane Newell [Veterinary Laboratories Agency (VLA), London], *C. jejuni* Δ*cgtA*/*neuB* were generated by insertion of a kanamycin-resistant cassette into the *cgtA*/*neuB* gene of 11168-O. *C. jejuni* Δ*waaF* and Δ*wlaA*-*wlaT* were obtained from Julian Ketley (University of Leicester, Leicester, UK) and transformed into *C. jejuni* 11168-O. *S. typhimurium* 180 and *S. typhimurium* 180 Δ*galE* was obtained from Ifor Beacham (Griffith University). *H. influenzae* 2019 and *H. influenzae* 2019 Δ*siaP* have been published (60).

S. flexneri and *S. typhimurium* were grown in lysogeny broth (10 g/L Tryptone, 5 g/L yeast extract, 5 g/L NaCl) with aeration for 16 h at 37 °C. Eighteen-hour cultures were diluted 1/20 into fresh broth and grown with aeration for 2 h at 37 °C to an optical density at 600 nm (OD_{600}) of ∼1. *S. flexneri* were collected (5×10^8) and washed twice with HBSS+ buffer [HBSS containing Ca^{2+} and Mg^{2+} supplemented with 10 mM Hepes; Sigma). *C. jejuni* was grown on Columbia blood agar and grown in microaerobic conditions at either 37 or 42 °C for 16 h. *H. influenzae* were grown as described by Johnston et al (60).

LPS/LOS Purification and Determination of LPS/LOS Concentration. LPS was purified from RMA2159, RMA2161, and RMA4328 as described by Darveau and Hancock (61), and hydrolyzed by heating in 1% (vol/vol) acetic acid for 90 min at 100 °C, followed by ultracentrifugation at 142,000 × *g* for 5 h at 4 °C. The supernatant containing the oligosaccharide was then freeze-dried and stored at 4 °C. LPS molarity concentration was determined by using the Purpald assay as described by Lee and Tsai (62), and 2-keto-3-deoxyoctonate was used to construct a standard curve. Oligosaccharide molarity concentration was determined by using the bicinchoninate assay as described by Doner and Irwin (63), and maltose was used to construct a standard curve. *C. jejuni* LOS was purified, hydrolyzed, and quantified as described in Semchenko et al. (59). *S. typhimurium* LPS was purified as described by Darveau and Hancock (61), and *H. influenzae* LPS was purified as described by Johnston et al. (60).

Glycan Array Analysis of Bacteria and Purified LOS/LPS. Glycan arrays were prepared as per Arndt et al (64). For whole bacteria, 10^6 cells were labeled with CFDA-SE, Bodipy 558-SE, or FITC for 30 min in 1× PBS with washing and application to the array performed as described by Day et al. (52).

FITC labeling and formalin fixing of *Shigella* strains was performed by pelleting 1×10^9/mL of bacteria and labeling with 0.5 mg/mL FITC (Sigma no. F4274) in 0.1 M sodium carbonate buffer (pH 9) for 2 h at room temperature, followed by several washes in 0.1 M sodium carbonate buffer (pH 9) to remove excess FITC, and then resuspended in PBS containing 2 mM $MgCl_2$, 2 mM $CaCl_2$ and 1% (wt/vol) paraformaldehyde.

LOS/LPS was labeled with lipophilic Bodipy methyl ester 595/625 as described in Semchenko et al. (65). Arrays were performed with 1 μg of LOS and rough mutant LPS or 10 μg of LPS with arrays performed as described in Semchenko et al (24). Scanning was performed by using a Proscan four laser Microarray scanner and the Scanarray express software. Yes/no binding was determined by four positive replicate spots in three replicate experiments. Positive binding was determined by spots being significantly greater than negative control spots by two-tailed *t* test in Microsoft Excel.

SPR Analysis of Glycan:Glycan Interactions of LOS/LOS. SPR was performed by using the Biacore T100 system and series S L1 sensor chips. LOS/LPS from

isolated from wild-type and rough mutant strains of *S. flexneri, C. jejuni, H. influenzae*, and *S. typhimurium* were captured onto the L1 chip at concentrations of 0.75 mg/mL and using unglycosylated lipid A from *E. coli* as the negative control on flow cell 1 as described in Semchenko et al (24). The running buffer used was 1× PBS (containing 2 mM $MgCl_2$, 2 mM $CaCl_2$) at a flow for analysis of 30 μL/min. A new layer of LOS/LPS/lipid A was captured for each sample. Single-cycle kinetics was used to generate the K_D of the interaction with each individual sugar concentration being optimized for the LOS/LPS used. Initial screening was done with 1:5 dilution series from 80 nM to 50 μM. Adjustments up or down in concentration were made before a 1:2 dilution series, completed using single-cycle kinetics using double referenced data (Dataset S2). All SPR experiments were performed a minimum of three times.

Modification of O-Deacylated LPS/LOS for SPR Analysis. LOS/LPS (500 μg) from *C. jejuni* 11168, *C. jejuni* 11168 Δ*waaF, H. influenzae* 2019, *H. influenzae* 2019 Δ*siaP, S. typhimurium* 180 and *S. typhimurium* 180 Δ*galE,* and *S. flexneri* RMA2159 and RMA2161 was O-deacylated as above, and the glycan only containing supernatant was freeze dried overnight. The dried glycan was resuspended to a final concentration of 20 μg/15 μL with 15 μL labeled with 2-aminobenzamide (2AB) through a Schiff's base reaction with sodium cyanoborohydride (25, 26). The free 2AB was removed from the samples by using GlycoProfile Glycan Clean-Up Cartridges.

SPR Analysis of Modified O-Deacylated LPS/LOS. O-deacylated LOS/LPS labeled with 2AB were immobilized onto a CM7 chip by using NHS/EDC coupling with 15 min of contact time at 5 μL/min flow rate with the remaining unreacted surface being blocked with ethanolamine. Between 80 and 200 response units of each bacterial glycan was immobilized to the surface with flow cell 1 on each chip being left as a blank ethanolamine surface as a control. Analytes were run in a 1:5 dilution series from 16 nM up to 10 μM by using single cycle kinetics with double-reference subtraction. All SPR experiments were performed in triplicate.

Isothermal Calorimetry Analysis of Glycan:Glycan Interactions. ITC was performed by using TA Instruments nano-ITC with the small (170 μL) capacity cell. The interaction was performed with a concentration of 0.2 M asialo-GM1 (Elicityl; GLY102) in the cell and 2 M blood group B tetrasaccharide (Elicityl; GLY038) in the syringe. A total of 20 injections of 2.5 μL were performed and interactions of both blood group B into PBS, and PBS injected into asialio-GM1 were run for subtraction. These subtractions runs were as follows: 2 M blood group B in PBS was injected in 20 injections of 2.5 μL into PBS buffer only; this data was then background subtracted from the B:GM1 interaction with injection per injection subtraction. Then PBS buffer only was injected into 0.2 M asialio-GM; measuring the changes in temperature caused by an injection of liquid into asialio-GM1 (dilution effects), providing a single value for subtraction. Analysis was performed by using the NanoAnalyze program (TA Instruments). K_D values were defined by using data from three independent experiments and displayed with an error of 1 SD.

Free Glycan Competition Assays of *C. jejuni* and *S. typhimurium* Infection of Caco-2 Monolayers and *S. flexneri* Infection of T84 Intestinal Epithelial Monolayers and Cell Association Studies of *H. influenzae* with 16HBE14 Bronchial Epithelial Cells. T84 intestinal epithelial cells were grown in 1:1 mixture of DMEM (Life Technologies no. 12430-054) and Ham's F-12 nutrient mixture (Life Technologies no. 11765-054) supplemented with 12.5 mM Hepes, 14 mM $NaHCO_3$, 10% (vol/vol) FCS, 100 U/mL penicillin/streptomycin, 8 μg/mL ampicillin, and 2 mM L-glutamine. Inverted monolayers were grown on 5 μM polycarbonate membrane inserts (Costar no. 3421, 24 well trays) precoated with 0.5 μg of rat tail collagen (Sigma no. C3867), and used 7–10 d after seeding (transwell media were refreshed every second day). A steady-state transepithelial cell resistance of ~800–1,500 $\Omega \cdot cm^2$ was reached in all monolayers used. Infection of T84 monolayers was performed as described by Kohler et al (2002) (11). Inverted T84 cell monolayers were washed twice with HBSS+ buffer, and bacterial samples were administrated to the basolateral surface of the T84 cell monolayer at an MOI of 25 bacteria per epithelial cell, followed by the addition of the required concentration of competing glycan. Infected monolayers were then incubated for 90 min at 37 °C with 5% CO_2, extensively washed (9×) and lysed with 1% (vol/vol) Triton X-100 in PBS. Viable counts were performed by plating onto LB agar and expressed as the number of adhered cells (CFU).

Caco-2 cells were grown in MEM and seeded for infection studies as described in Day et al. (2009) with *C. jejuni* grown at 42 °C (52). *S. typhimurium* was added at an MOI of 100 bacteria per epithelial cell, and infected monolayers were then incubated for 30 min at 37 °C with 5% CO_2, washed (three times) and lysed with 1% (vol/vol) Triton X-100 in PBS. Viable counts were performed by plating onto LB agar and expressed as the number of adhered cells (CFU). Competing glycans were added at listed concentrations, and the infection was carried out for 30 min. Cells washed and lysed and the CFU determined as per Day et al (52).

Human bronchial epithelial cells 16HBE14 were cultured as described (66). Infection was carried out with 1×10^7 CFU of *H. influenzae* and Δ*siaP* mutant on 1×10^5 confluent 6HBE14 bronchial epithelial cells in 24-well plates. Two-hour association assays were performed in a 1-mL volume, wash three times in 1 mL of PBS after 2 h of association time, lysed in 5% saponin, and viable counts were performed and cell numbers were expressed as a percentage of the original inoculums.

Conjugation of *S. flexneri* O-Deacylated Polysaccharide with Alexa 488. O-deacylated *S. flexneri* LPS (25 μM) was mixed with 10 μM Alexa 488 hydroxylamine (Life Technologies no. A30629) and 100 mM aniline in 0.1 M sodium phosphate buffer (pH 7.0), followed by incubation at room temperature for 16 h (covered in foil). The labeled conjugate mix was then dialyzed against 5 L of MQ water twice over a 24-h period to remove unconjugated Alexa 488 hydroxylamine reagent. The resultant fluorescent Alexa 488-polysaccharide conjugate was stored at −20 °C until use.

Staining of Human Ileum Sections with *S. flexneri* Alexa-488 Polysaccharide and Immunofluorescence Staining. Paraffin embedded human ileum sections sourced from Zyagen (no. HP-311) were rehydrated, blocked with 10% (vol/vol) FCS, and incubated with Alexa 488-polysaccharide conjugate (~10 μM) and monoclonal anti-GP2 antibodies (MBL) (1:500) for 30 min at 37 °C. Sections were then washed three times with PBS, incubated with Alexa 594-conjugated donkey anti-mouse secondary antibodies (Molecular Probes) (1:100) for 1 h at 37 °C, and rewashed with PBS. Cellular nuclei in the section was counterstained with 0.1 μg/mL 4,6-diamidino-2-phenylindole (DAPI) (Sigma). Sections were mounted with square coverslips by using Mowiol 4-88 (Calbiochem) containing 20 μg/mL *p*-phenylenediamine (Sigma) and examined with an Olympus IX-70 microscope with phase-contrast optics using 4× objective and 40× oil immersion objective. Fluorescence and phase contrast images were captured and false color merged by using Metamorph software program (version 7.7.1.0; Molecular Devices).

ACKNOWLEDGMENTS. This work was supported by National Health and Medical Research Council Program Grant 565526 (to M.P.J. and R.M.); a Smart Futures Fund Research Partnerships Program Grant (to M.P.J.); a Helen C. Levitt Visiting Professorship, The University of Iowa (M.P.J.); and Grant AI024616 from National Institute of Allergy and Infectious Diseases, Public Health Service (to M.A.A.).

1. Lehmann F, Tiralongo E, Tiralongo J (2006) Sialic acid-specific lectins: Occurrence, specificity and function. *Cell Mol Life Sci* 63(12):1331–1354.
2. Sokurenko EV, et al. (1998) Pathogenic adaptation of Escherichia coli by natural variation of the FimH adhesin. *Proc Natl Acad Sci USA* 95(15):8922–8926.
3. Gilboa-Garber N, Sudakevitz D (1999) The hemagglutinating activities of Pseudomonas aeruginosa lectins PA-IL and PA-IIL exhibit opposite temperature profiles due to different receptor types. *FEMS Immunol Med Microbiol* 25(4): 365–369.
4. Ilver D, et al. (1998) Helicobacter pylori adhesin binding fucosylated histo-blood group antigens revealed by retagging. *Science* 279(5349):373–377.
5. Mahdavi J, et al. (2002) Helicobacter pylori SabA adhesin in persistent infection and chronic inflammation. *Science* 297(5581):573–578.
6. Handa K, et al. (2007) Le(x) glycan mediates homotypic adhesion of embryonal cells independently from E-cadherin: A preliminary note. *Biochem Biophys Res Commun* 358(1):247–252.
7. Popescu O, Checiu I, Gherghel P, Simon Z, Misevic GN (2003) Quantitative and qualitative approach of glycan-glycan interactions in marine sponges. *Biochimie* 85(1-2): 181–188.
8. Moran AP, Gupta A, Joshi L (2011) Sweet-talk: Role of host glycosylation in bacterial pathogenesis of the gastrointestinal tract. *Gut* 60(10):1412–1425.
9. Yamaoka Y (2008) Roles of Helicobacter pylori BabA in gastroduodenal pathogenesis. *World J Gastroenterol* 14(27):4265–4272.
10. Jacques M (1996) Role of lipo-oligosaccharides and lipopolysaccharides in bacterial adherence. *Trends Microbiol* 4(10):408–409.
11. Köhler H, Rodrigues SP, McCormick BA (2002) Shigella flexneri interactions with the basolateral membrane domain of polarized model intestinal epithelium: Role of lipopolysaccharide in cell invasion and in activation of the mitogen-activated protein kinase ERK. *Infect Immun* 70(3):1150–1158.
12. Cohen PS, Arruda JC, Williams TJ, Laux DC (1985) Adhesion of a human fecal Escherichia coli strain to mouse colonic mucus. *Infect Immun* 48(1):139–145.

13. Gupta SK, Berk RS, Masinick S, Hazlett LD (1994) Pili and lipopolysaccharide of Pseudomonas aeruginosa bind to the glycolipid asialo GM1. *Infect Immun* 62(10): 4572–4579.
14. Izhar M, Nuchamowitz Y, Mirelman D (1982) Adherence of Shigella flexneri to guinea pig intestinal cells is mediated by a mucosal adhesion. *Infect Immun* 35(3): 1110–1118.
15. McSweegan E, Walker RI (1986) Identification and characterization of two Campylobacter jejuni adhesins for cellular and mucous substrates. *Infect Immun* 53(1): 141–148.
16. Mroczenski-Wildey MJ, Di Fabio JL, Cabello FC (1989) Invasion and lysis of HeLa cell monolayers by Salmonella typhi: The role of lipopolysaccharide. *Microb Pathog* 6(2): 143–152.
17. Palomar J, Leranoz AM, Viñas M (1995) Serratia marcescens adherence: The effect of O-antigen presence. *Microbios* 81(327):107–113.
18. Pier GB, et al. (1996) Role of mutant CFTR in hypersusceptibility of cystic fibrosis patients to lung infections. *Science* 271(5245):64–67.
19. Tang HB, et al. (1996) Contribution of specific Pseudomonas aeruginosa virulence factors to pathogenesis of pneumonia in a neonatal mouse model of infection. *Infect Immun* 64(1):37–43.
20. Valkonen KH, Wadström T, Moran AP (1994) Interaction of lipopolysaccharides of Helicobacter pylori with basement membrane protein laminin. *Infect Immun* 62(9): 3640–3648.
21. Chowers Y, et al. (2007) O-specific [corrected] polysaccharide conjugate vaccine-induced [corrected] antibodies prevent invasion of Shigella into Caco-2 cells and may be curative. *Proc Natl Acad Sci USA* 104(7):2396–2401.
22. Nishiuchi Y, Doe M, Hotta H, Kobayashi K (2000) Structure and serologic properties of O-specific polysaccharide from Citrobacter freundii possessing cross-reactivity with Escherichia coli O157:H7. *FEMS Immunol Med Microbiol* 28(2):163–171.
23. Paton AW, Voss E, Manning PA, Paton JC (1998) Antibodies to lipopolysaccharide block adherence of Shiga toxin-producing Escherichia coli to human intestinal epithelial (Henle 407) cells. *Microb Pathog* 24(1):57–63.
24. Semchenko EA, et al. (2012) Structural heterogeneity of terminal glycans in Campylobacter jejuni lipooligosaccharides. *PLoS One* 7(7):e40920.
25. Hermanson GT (1996) *Bioconjugate Techniques* (Academic, New York), 1st Ed.
26. Lane CF (1975) Sodium cyanoborohydride - highly selective reducing agent for organic functional groups. *Synthesis-Stuttgart* 8(3):135–146.
27. Amano J, Oshima M (1999) Expression of the H type 1 blood group antigen during enterocytic differentiation of Caco-2 cells. *J Biol Chem* 274(30):21209–21216.
28. Ou G, Baranov V, Lundmark E, Hammarström S, Hammarström ML (2009) Contribution of intestinal epithelial cells to innate immunity of the human gut–studies on polarized monolayers of colon carcinoma cells. *Scand J Immunol* 69(2):150–161.
29. Arena ET, et al. (2015) Bioimage analysis of Shigella infection reveals targeting of colonic crypts. *Proc Natl Acad Sci USA* 112(25):E3282–E3290.
30. Sansonetti PJ, Tran Van Nhieu G, Egile C (1999) Rupture of the intestinal epithelial barrier and mucosal invasion by Shigella flexneri. *Clin Infect Dis* 28(3):466–475.
31. Komorowski L, et al. (2013) Autoantibodies against exocrine pancreas in Crohn's disease are directed against two antigens: The glycoproteins CUZD1 and GP2. *J Crohn's Colitis* 7(10):780–790.
32. Sharma R, Schumacher U (2001) Carbohydrate expression in the intestinal mucosa. *Adv Anat Embryol Cell Biol* 160:III–IX, 1–91.
33. Sharma R, Schumacher U, Adam E (1998) Lectin histochemistry reveals the appearance of M-cells in Peyer's patches of SCID mice after syngeneic normal bone marrow transplantation. *J Histochem Cytochem* 46(2):143–148.
34. Misevic GN (1999) Molecular self-recognition and adhesion via proteoglycan to proteoglycan interactions as a pathway to multicellularity: Atomic force microscopy and color coded bead measurements in sponges. *Microsc Res Tech* 44(4):304–309.
35. de la Fuente JM, Penadés S (2004) Understanding carbohydrate-carbohydrate interactions by means of glyconanotechnology. *Glycoconj J* 21(3-4):149–163.
36. Pérez S (1994) *The Structure of Sucrose in the Crystal and in Solution Sucrose: Properties and Applications*, eds Mathlouthi M, Reiser P (Springer Science and Business Media, Dordrecht, The Netherlands).
37. Mcdonald TRR, Beevers CA (1952) The crystal and molecular structure of alpha-glucose. *Acta Crystallogr* 5(5):654–659.
38. Sikorski P, Hori R, Wada M (2009) Revisit of alpha-chitin crystal structure using high resolution X-ray diffraction data. *Biomacromolecules* 10(5):1100–1105.
39. Beevers CA, Hansen HN (1971) Structure of alpha-lactose monohydrate. *Acta Crystall B* 27(Jul15):1323–1325.
40. Murray GL, Attridge SR, Morona R (2003) Regulation of Salmonella typhimurium lipopolysaccharide O antigen chain length is required for virulence; identification of FepE as a second Wzz. *Mol Microbiol* 47(5):1395–1406.
41. Bouchet V, et al. (2003) Host-derived sialic acid is incorporated into Haemophilus influenzae lipopolysaccharide and is a major virulence factor in experimental otitis media. *Proc Natl Acad Sci USA* 100(15):8898–8903.
42. Naito M, et al. (2010) Effects of sequential Campylobacter jejuni 81-176 lipooligosaccharide core truncations on biofilm formation, stress survival, and pathogenesis. *J Bacteriol* 192(8):2182–2192.
43. Phalipon A, et al. (1995) Monoclonal immunoglobulin A antibody directed against serotype-specific epitope of Shigella flexneri lipopolysaccharide protects against murine experimental shigellosis. *J Exp Med* 182(3):769–778.
44. Hong M, Payne SM (1997) Effect of mutations in Shigella flexneri chromosomal and plasmid-encoded lipopolysaccharide genes on invasion and serum resistance. *Mol Microbiol* 24(4):779–791.
45. Morona R, Daniels C, Van Den Bosch L (2003) Genetic modulation of Shigella flexneri 2a lipopolysaccharide O antigen modal chain length reveals that it has been optimized for virulence. *Microbiology* 149(Pt 4):925–939.
46. Van den Bosch L, Manning PA, Morona R (1997) Regulation of O-antigen chain length is required for Shigella flexneri virulence. *Mol Microbiol* 23(4):765–775.
47. Mabbott NA, Donaldson DS, Ohno H, Williams IR, Mahajan A (2013) Microfold (M) cells: Important immunosurveillance posts in the intestinal epithelium. *Mucosal Immunol* 6(4):666–677.
48. Giannasca PJ, Giannasca KT, Falk P, Gordon JI, Neutra MR (1994) Regional differences in glycoconjugates of intestinal M cells in mice: Potential targets for mucosal vaccines. *Am J Physiol* 267(6 Pt 1):G1108–G1121.
49. Prieto PA, et al. (1997) Expression of human H-type alpha1,2-fucosyltransferase encoding for blood group H(O) antigen in Chinese hamster ovary cells. Evidence for preferential fucosylation and truncation of polylactosamine sequences. *J Biol Chem* 272(4):2089–2097.
50. Kanipes MI, et al. (2008) Genetic analysis of lipooligosaccharide core biosynthesis in Campylobacter jejuni 81-176. *J Bacteriol* 190(5):1568–1574.
51. Kanipes MI, Holder LC, Corcoran AT, Moran AP, Guerry P (2004) A deep-rough mutant of Campylobacter jejuni 81-176 is noninvasive for intestinal epithelial cells. *Infect Immun* 72(4):2452–2455.
52. Day CJ, et al. (2009) Differential carbohydrate recognition by Campylobacter jejuni strain 11168: Influences of temperature and growth conditions. *PLoS One* 4(3):e4927.
53. Levy P, Robert A, Picard J (1988) Biosynthesis of glycosaminoglycans in the human colonic tumor cell line Caco-2: Structural changes occurring with the morphological differentiation of the cells. *Biol Cell* 62(3):255–264.
54. Ruiz-Palacios GM, Cervantes LE, Ramos P, Chavez-Munguia B, Newburg DS (2003) Campylobacter jejuni binds intestinal H(O) antigen (Fuc alpha 1, 2Gal beta 1, 4GlcNAc), and fucosyloligosaccharides of human milk inhibit its binding and infection. *J Biol Chem* 278(16):14112–14120.
55. Murray GL, Attridge SR, Morona R (2006) Altering the length of the lipopolysaccharide O antigen has an impact on the interaction of Salmonella enterica serovar Typhimurium with macrophages and complement. *J Bacteriol* 188(7):2735–2739.
56. al-Bahry SN, Pistole TG (1997) Adherence of Salmonella typhimurium to murine peritoneal macrophages is mediated by lipopolysaccharide and complement receptors. *Zentralbl Bakteriol* 286(1):83–92.
57. Jan KM, Chien S (1973) Role of surface electric charge in red blood cell interactions. *J Gen Physiol* 61(5):638–654.
58. Kojima N, Shiota M, Sadahira Y, Handa K, Hakomori S (1992) Cell adhesion in a dynamic flow system as compared to static system. Glycosphingolipid-glycosphingolipid interaction in the dynamic system predominates over lectin- or integrin-based mechanisms in adhesion of B16 melanoma cells to non-activated endothelial cells. *J Biol Chem* 267(24):17264–17270.
59. Semchenko EA, et al. (2010) Temperature-dependent phenotypic variation of Campylobacter jejuni lipooligosaccharides. *BMC Microbiol* 10:305.
60. Johnston JW, et al. (2008) Characterization of the N-acetyl-5-neuraminic acid-binding site of the extracytoplasmic solute receptor (SiaP) of nontypeable Haemophilus influenzae strain 2019. *J Biol Chem* 283(2):855–865.
61. Darveau RP, Hancock RE (1983) Procedure for isolation of bacterial lipopolysaccharides from both smooth and rough Pseudomonas aeruginosa and Salmonella typhimurium strains. *J Bacteriol* 155(2):831–838.
62. Lee CH, Tsai CM (1999) Quantification of bacterial lipopolysaccharides by the purpald assay: Measuring formaldehyde generated from 2-keto-3-deoxyoctonate and heptose at the inner core by periodate oxidation. *Anal Biochem* 267(1):161–168.
63. Doner LW, Irwin PL (1992) Assay of reducing end-groups in oligosaccharide homologues with 2,2′-bicinchoninate. *Anal Biochem* 202(1):50–53.
64. Arndt NX, Tiralongo J, Madge PD, von Itzstein M, Day CJ (2011) Differential carbohydrate binding and cell surface glycosylation of human cancer cell lines. *J Cell Biochem* 112(9):2230–2240.
65. Semchenko EA, Moutin M, Korolik V, Tiralongo J, Day CJ (2012) Lectin array analysis of purified lipooligosaccharide: A method for the determination of molecular mimicry. *J Glycomics Lipidomics* 02:103.
66. Swords WE, et al. (2000) Non-typeable Haemophilus influenzae adhere to and invade human bronchial epithelial cells via an interaction of lipooligosaccharide with the PAF receptor. *Mol Microbiol* 37(1):13–27.